JOURNAL OF AIRCRAFT
Vol. 45, No. 5, September–October 2008

Stereo Projections of Miss Distance in Some New Cockpit Display Formats

D. J. Gates,* E. A. Gates,* M. Westcott,* and N. L. Fulton*
Commonwealth Scientific and Industrial Research Organisation, Canberra, Australian Capital Territory 2601, Australia

DOI: 10.2514/1.35574

The design basis of new display formats for multifunction and head-up displays is described. The purpose of the formats is to provide pilots with an immediate visualization of the potential danger of a midair collision. These formats incorporate adaptations of steering and guidance concepts used in the cockpit displays of military aircraft and consist of stereographic projections of critical directions around own aircraft. One type of multifunction format is a color image, in which color indicates the expected miss distance from another aircraft for all hypothetical flight-path directions of own aircraft. It resembles a topographic map and enables a pilot to steer for the safe "valleys" and avoid the dangerous "peaks" that represent collisions. It thereby combines orientation information, as in the vertical situation display, with path information, as in the navigation display. In the complementary head-up format, a line plot of contours of constant miss distance serves as a monochrome display. The new display formats contain the essential three-dimensional information, unlike the current traffic alert and collision avoidance system displays, but do not have the complexity of three-dimensional perspective displays. Images are shown from a computer program that simulates the flight of the aircraft and generates the displays in the form of interactive animation. The aircraft paths can be set from input files or own aircraft can be flown manually from the keyboard, thereby enabling an engineering evaluation of the displays. Measures of the effectiveness of the format are evaluated using computer simulations based on a model of pilot responses.

Nomenclature

h	=	distance of a point from the vertex of the cone in the x direction
$h_+(\phi)$	=	solution of Eq. (B8), $h_-(\phi)$ is the other solution
R_{CPA}	=	separation at closest point of approach
R_{MD}	=	3-D expected miss distance between own aircraft and intruder
R_0	=	current 3-D distance between own aircraft and intruder
t_{CPA}	=	time until closest point of approach
$\bar{\mathbf{U}}_F$	=	unit vector in the hypothetical direction of own aircraft
$\mathbf{U}_{\mathrm{LOS}}$	=	unit vector from own aircraft to intruder
$\mathbf{U}_R$	=	unit vector parallel to $\mathbf{V}_R$
V_F	=	speed of own aircraft
$\mathbf{V}_F$	=	velocity vector of own aircraft
$\bar{\mathbf{V}}_F$	=	hypothetical velocity vector of own aircraft
$\mathbf{V}_R$	=	velocity vector of own aircraft relative to intruder
V_{Rx}	=	x component of $\mathbf{V}_R$, similarly for V_{Ry} and V_{Rz}
V_T	=	speed of intruder
$\mathbf{V}_T$	=	velocity vector of intruder
V_{Tx}	=	x component of $\mathbf{V}_T$, similarly for V_{Ty} and V_{Tz}
X	=	x component of $\bar{\mathbf{V}}_F$, similarly for Y and Z
x	=	coordinate parallel to $\mathbf{U}_{\mathrm{LOS}}$
y	=	coordinate perpendicular to $\mathbf{U}_{\mathrm{LOS}}$ in the plane of $\mathbf{U}_{\mathrm{LOS}}$ and $\mathbf{V}_T$
z	=	coordinate perpendicular to x and y
β	=	$\tan\theta$
θ	=	semi-angle of cone of directions
ϕ	=	polar angle of a point around the axis of the cone

Received 8 November 2007; revision received 31 January 2008; accepted for publication 2 February 2008.

*Research Scientist, Mathematical and Information Sciences, General Post Office Box 664.

I. Introduction

AS A last line of defense in many situations in air traffic management (ATM) systems, the traffic alert and collision avoidance system (TCAS-II) and its associated displays have served commercial aviation well for several decades. In the near future it will become feasible, and perhaps necessary, to place greater reliance on enhanced TCAS-type systems. The feasibility arises from advances in air-to-air (A/A) data links (e.g., automatic dependent surveillance–broadcast, or ADS-B) and onboard navigation systems, including the global positioning system (GPS). Such needs arise as ATM systems face ever-increasing traffic flow rates. The limitations of the current TCAS-II for this role have been widely discussed [1–6]. The TCAS-II traffic display shows only the current position, altitude, and altitude rate of the intruder and threat aircraft. The conflict resolution commands from the TCAS-II are to climb or descend only. Advice is not given to turn, because the horizontal relative position is not known with enough accuracy to provide reliable advice, but such changes [7] are envisaged in systems such as the TCAS-IV. These changes are needed in many situations in which vertical maneuvers are restricted by other traffic, ground proximity, weather, or other operational factors [1,8]. These deficiencies are most evident in close encounters in which normal routing and avoidance might have failed due to human error or unforeseen circumstances or where close maneuvering is required at an airport [6,9]. Consequently, much research [5,10] has been devoted to designing displays that provide greater situational awareness for pilots and improve their confidence in extended proximity management. For example, the cockpit displays for traffic information (CDTI) provide an approach to an overall architecture inclusive of such issues. Concepts of proximity management and display design are discussed further in Sec. VI. Some readers might like to read Sec. VI at this point but will find it to be clearer after reading about the new concept.

This paper presents a new design (Australian provisional patent number 2006900884, international patent pending) based on proven techniques and format symbology that have long been used in military aircraft. The military A/A systems and the A/A radar display [11–13] (AARD) are sophisticated and powerful means of informing pilots during close A/A combat [14]. Figure 1 is a sketch of a key

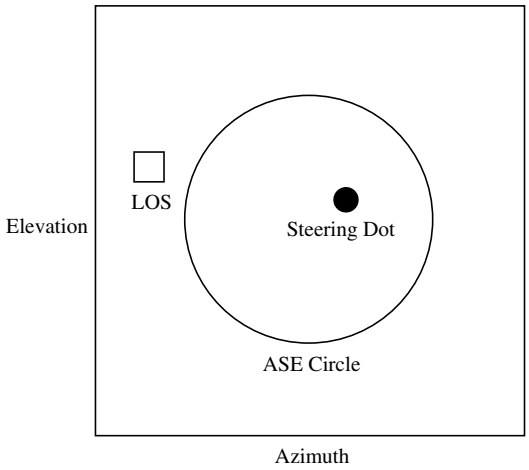

Fig. 1 A sketch of the air-to-air radar display in fighter aircraft, showing only features of interest here. The ranges of azimuth and elevation can be selected by the pilot.

feature of the AARD. When a target is out of range, the display simply directs own aircraft on a collision course with the target. The pilot can achieve this by steering so that the steering dot is centered in the display. It is easy to see that this might form the basis of a civil format (that augments a display architecture such as CDTI) in which the pilot's objective would be to *avoid* centering the dot. The AARD is essentially a Mercator projection [15] of the front rectangle of the directions scanned by own aircraft's sensors (this information can be presented like the familiar contours in an aeronautical chart or a weather radar display). In this projection, a direction in 3-D space becomes a point in the 2-D display. The line of sight (LOS) of the target becomes a point, represented by a square centered on that point (Fig. 1). The allowed steering error (ASE) circle indicates a range of possible steering directions; when the steering dot lies inside the circle, an intercept is possible. In the proximity management context, this is a circumstance to avoid. As mentioned, it will soon become technically possible to provide display formats based on similar principles in civil aircraft, with the capability of avoiding conflicting flight paths. Automated guidance via these principles is a further possibility (Sec. V).

To create a civil display format, one needs to supplement the information in Fig. 1 with a suitable calibration of the level of danger. The ASE circle is suggestive here. For out-of-range threats, it has a small, fixed angular radius. Hence, the radial position of the dot relative to the circumference gives an indication of the expected or extrapolated miss distance (EMD) (or minimum separation) of the two aircraft for their current speeds and directions. The EMD is critical information for pilots and is difficult for pilots to estimate, and so it is desirable to display this more directly and clearly. The new format shows values of the EMD for all relevant steering directions (see the right-hand side of Fig. 2) as explained in Sec. II. Then, pilots can steer to increase the EMD for the greatest threat while allowing for other possible conflicts. Although the existing TCAS displays show the present situation, the new display also shows the possible futures and enables pilots to choose a safe future. The display updates continuously, and so the consequences of changing aircraft positions and maneuvers are continuously visible. Thus, the display is a distillation of the essential 3-D information of the type currently available in military aircraft.

One version of the format is a color-coded multifunctional display (MFD) shown in Figs. 2 and 3 (right-hand side). Another version is a simpler line plot (Figs. 4 and 5), which could be added to the vertical situation display (VSD) or to a head-up display (HUD) form of VSD. As is well known, a HUD is valuable in critical situations and in times of heavy pilot workload [11,16–18]. These displays are demonstrated in the present work via a computer animation that simulates the motion of aircraft. Figure 2 is a typical screen snapshot of this animation; the contents of the screen are described later. A number of natural variants and their particular merits are also outlined.

As mentioned, the basic display principle of Fig. 1 has long been proven in military aircraft. To supplement this evidence, the new formats are evaluated by carrying out a large number of simulations of conflict situations using a natural model of pilot responses to the displays. Some performance metrics are evaluated. The model pilot response leads to avoidance maneuvers that, coincidentally, are

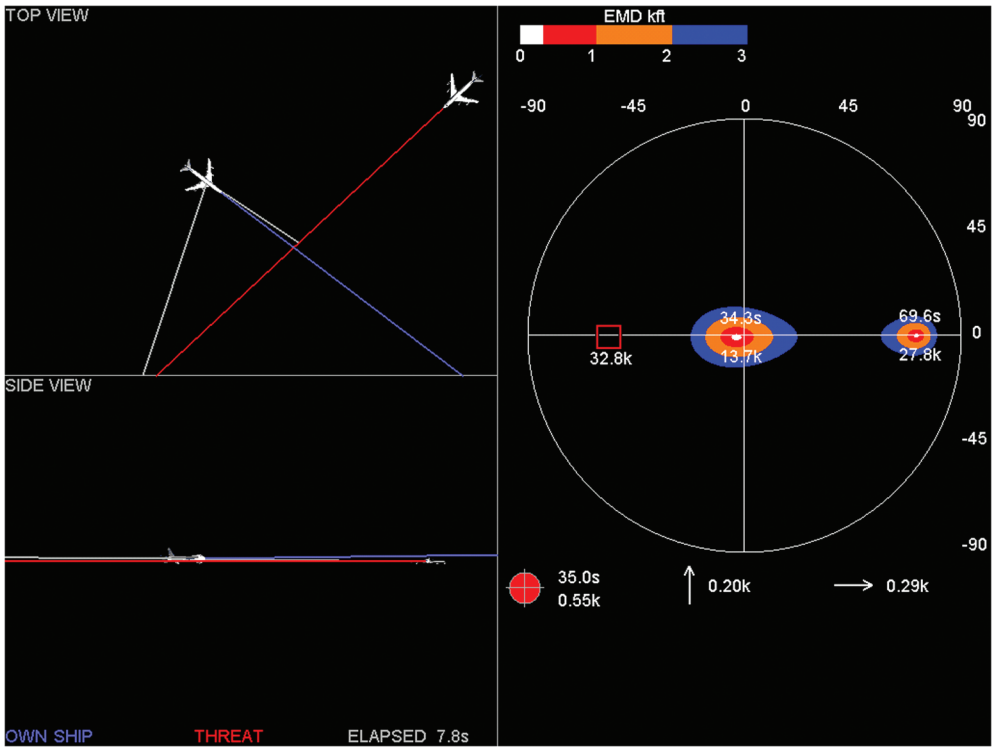

Fig. 2 A screen from the computer animation showing a case in which there are two collision directions for own aircraft. These are indicated by the two gray lines in the left box and correspond to the centers of the white zones in the display. The white zone below and to the left of own aircraft is the main concern.

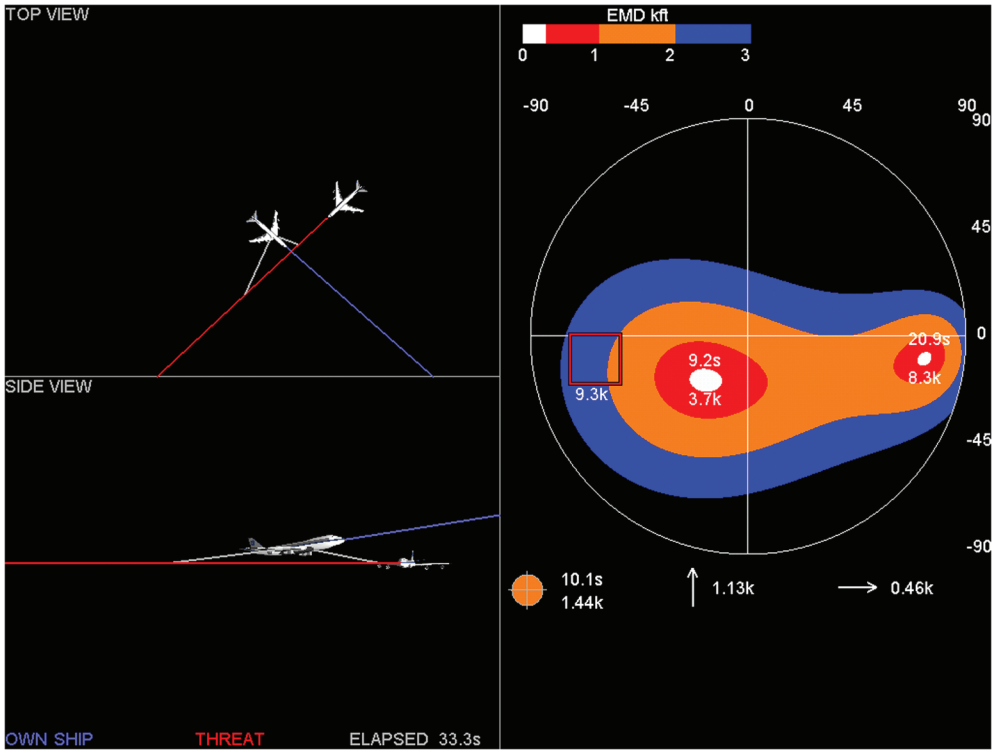

Fig. 3 Resolution of the conflict shown in Fig. 2. Own aircraft has climbed to achieve a miss distance of 1440 ft. Note that, compared with Fig. 2, the symbols and colored zones are much larger, an automatic consequence of the aircraft being closer. Thus the proximity is more obvious to the own aircraft pilot.

similar to those suggested by Gazit and Powell [19] and developed by Zeghal [20]. The display format has been examined by several pilots with differing backgrounds (see Acknowledgements), including coauthor N. L. Fulton. The issue of performing formal trials with pilots at this stage of engineering development is discussed in Sec. VI.

The current paper concentrates on explaining the essential architecture of the display formats. Readers with experience in the field will recognize how details can be modified or added and how human factor considerations could be integrated into an overall display design. Section II describes Fig. 2 and the color format in detail. Section III describes how the format information helps to resolve a conflict. Section IV describes the HUD format. Section V describes the simulation study. Section VI reviews some display formats proposed by others and discusses the new format in a more general context. Section VII gives conclusions and mentions some extensions of the work. Appendix A gives the vector formulas for collision directions and EMDs. Appendix B gives the equations for the EMD contours and classifies their possible shapes.

II. Multifunctional Display Format and the Screen Generated by the Computer Simulation

Here the computer simulation screen in Fig. 2 is explained. The right half of the screen shows the format for the cockpit display. The left half of the screen shows the aircraft situation and is *not part of the proposed cockpit display* format; some situational information of this type is available in current plan view navigation (NAV) displays and in other proposed formats such as CDTI. The situation has the following parameters: own aircraft speed, 400 ft/s; intruder speed, 780 ft/s; and both aircraft flying level and own aircraft 200 ft higher than the intruder.

A. Plan View from Above

The top left box in Fig. 2 shows a plan view of two aircraft on a near-collision course. They are computer graphic models of two Boeing 747s, but any type of aircraft could be represented. The aircraft images are magnified and the whole scene is shown in perspective, and so higher aircraft appear larger. A colored line shows the direction of the current velocity vector of each aircraft projected on the plane: blue for own aircraft and red for the intruder. The gray lines emanating from own aircraft show the directions that would lead to collisions and are therefore to be avoided. They are calculated on the basis that neither aircraft changes speed and the intruder continues with its current velocity vector. There are two 3-D collision directions because the intruder is faster and the aircraft are closing. The directions and their calculation are explained in Appendix A. The directions change dynamically as aircraft positions and velocity vectors change with time. If the intruder were slower than own aircraft, there would be at most one collision direction.

The underlying aircraft simulator is essentially a point mass model with 3 degrees of freedom (3 DOF). The bank angle while turning is determined by the standard force balance. Simulated aircraft paths can be created as input files, or own aircraft can be flown from the keyboard. Aircraft can climb, descend, speed up, slow down, and turn. One can pause and continue the program and one can zoom in or out. These features enable one to evaluate the formats and demonstrate their use to pilots and industry representatives. A future development would be to incorporate realistic aircraft simulations with 6 degrees of freedom for each type of aircraft, but that would complicate the present exposition of the display design.

B. Side View

The bottom left box in Fig. 2 duplicates the same situation observed from the side corresponding to the bottom edge of the plan view. It is also a perspective scene. The elapsed time of the simulation is shown at the bottom.

C. Front Hemisphere Projection

The right-hand side of Fig. 2 is one version of an MFD format. The disk is a zenithal projection [4] of the front hemisphere of the directions around own aircraft, in which the zenith is directly ahead of own aircraft. The familiar VSD is such a projection. The crosshairs are aligned with the own aircraft body axes. The center of the front projection corresponds to the longitudinal body axis of own aircraft, or the pilot's viewpoint straight ahead. In the present 3 DOF model,

the latter direction coincides with the flight path, and so an angle of attack is not included at this stage. This angle is typically small in large passenger aircraft. The equal radial angles in 3-D, relative to the central directions, are represented as equal radial distances from the centers of the projections. The circumference of the circle is at 90 deg from the center and represents the directions lying in a plane through the pilot and normal to own aircraft's longitudinal body axis.

The LOS, giving the 3-D direction of the intruder from own aircraft, is shown as a hollow red square. This modified TCAS symbol has been suggested ([16], Fig. 2) for the resolution advisory mode as it causes less occlusion than the solid square currently used. A hollow square is also the AARD symbol ([13], Fig. 51). The size of the square varies continuously to indicate the distance to the intruder, but its minimum size is fixed. This is designed to provide a visual impression of closer intruders but to maintain an awareness of aircraft at a longer range.

The colored zones are a representation of the EMD, or the expected minimum physical separation, between own aircraft and the intruder for all hypothetical own aircraft flight-path directions. To explain the bands, let us choose a hypothetical direction for own aircraft. Now, suppose own aircraft were on this flight path with its current speed. Suppose that the intruder continues with its current velocity vector. On this basis, a hypothetical EMD is calculated (Appendix A). One chooses the color from the legend appropriate for this distance and colors the screen pixel at this point accordingly. If the EMD is beyond the nominated range of the legend, which is 3 kft in this case (Fig. 2), then the pixel is left black. In this way, the display is colored so as to show an EMD for a continuum of hypothetical flight-path directions for own aircraft. In this instance, the blue zone represents EMDs in the range of 2–3 kft, yellow/amber represents 1–2 kft, and red represents 1 kft–300 ft, as the legend indicates. The color sequence is in accordance with the colors used in TCAS for the different levels of alert and advisory symbols. In this instance, the bright white collision zones correspond to EMDs of less than 300 ft and could result in a wing-tip collision between two large aircraft with such a wing span. They are projections of the collision directions shown on the left half of the screen, expanded to represent the dimensions of the aircraft. White is chosen here for its visual prominence. The closer collision zone is the analog of the steering dot in Fig. 1.

The EMD is a possible measure of safety for that direction. From the display, the pilot can immediately evaluate a level of safety or danger associated with any steering direction. The aim is to then steer so as to ensure an adequate ultimate miss distance, so that the aircraft is steered away from the white peaks and toward the black valleys, as if the display were a topographic map. In Fig. 2, own aircraft is steering very close to the collision zone but slightly to the right of and above it. This is a dangerous conflict and Sec. III shows how it is resolved.

The size of the colored zones increases as the aircraft come closer, as shown in Fig. 3. This has two desirable properties. First, the larger zones create a greater visual impression of danger when it is appropriate. Second, it directly conveys the information that own aircraft's safe steering directions are more extreme and require more urgent action. Likewise in the AARD, the ASE circle grows as one closes in on an in-range target. In some circumstances, such as a retreating intruder, there is no collision zone. But the colored zones might still be present, possibly with some inner colors missing (see Appendix B).

More than one intruder may be displayed. Usually they will not be in close encounters with own aircraft, and so their symbols and colored zones will be small. Then, the display provides situational information about intruder bearings, through their LOSs, and about possible, nonurgent conflicts. The zones will grow significantly, and alerts commence, only during a close encounter. In the unlikely event that two intruders are involved, their colored zones could overlap. Then, a pixel would potentially have different colors for two intruders, and so it is assigned the color of the smaller EMD, as in [11].

Other information, such as a horizon, can be readily added to the display format.

D. Conflict Data

The display in Fig. 2 shows data for an intruder in a close encounter. If there are two such intruders, the data for the greater threat are displayed. The current distance of the intruder is attached to the LOS symbol. The current distance and time to the collision points are attached to the collision zones.

Three symbols are shown below the main disk:

1) On the left is a small disk, whose color is the same as the center of the display, with the current direction of own aircraft. The time and distance to the closest approach are shown alongside this disk. When the aircraft are receding, their current separation is shown.

2) In the middle is a vertical arrow that can point up or down to indicate whether to climb or descend. The upward arrow in Fig. 2 indicates that own aircraft will cross above the intruder in this case, and so climbing will improve separation. The number gives the value, H_M, of the vertical component of the EMD in kilofeet (Appendix A). A downward pointing arrow would indicate that own aircraft will cross below the intruder.

3) On the right is a horizontal arrow that can point left or right to indicate how to turn. The rightward arrow in Fig. 2 indicates that own aircraft will cross to the right of the intruder in this case, and so turning right will improve separation. The number gives the value, W_M, of the horizontal component of the EMD in kilofeet (Appendix A). A leftward pointing arrow would indicate that own aircraft will cross to the left of the intruder. Consequently, the directions of the arrows indicate how own aircraft should steer to increase either component of the EMD, which reinforces the visual evidence of the displays. The arrows vanish when the aircraft are receding.

E. Further Comments

Obviously, there is no perfect projection of the whole sphere of directions, just as there is no perfect map of the world. The front hemisphere zenithal projection provides the least overall distortion of angles. The Mercator projection is an alternative. The range of angles in any of the projections could be limited to show small angle changes, as in the track-while-scan [13] mode of the AARD. The range of EMDs in the color scale could be changed. The scale could be selected by the pilot or according to an algorithm. This would allow finer resolution of separations when the aircraft are dangerously close (as in Sec. V). The colored conflict band, described by Barhydt and Hansman [3], is another way of indicating a computed miss distance. Their directional information is related mainly to known changes in the direction of the intruder. The present purpose is to inform own aircraft, more directly, about the consequences of changing its own direction while the display continually responds to any action by the intruder.

III. Using the Display to Resolve a Conflict

Figure 2 shows that the aircraft will miss by only 550 ft in 35.0 s if both aircraft hold their directions and speeds exactly. The pilot of own aircraft sees the main collision point nearly straight ahead and sees the red color at the current flight-path direction and also in the data box. Minor drifts in direction could lead to a collision. The arrows in the data box indicate that, at minimum separation, own aircraft will be 200 ft above the intruder and 290 ft in front.

It is assumed there is other traffic below, preventing a descent by either aircraft. Own aircraft would commonly turn to the right, which the display supports. But if the intruder continues on its direction, there is the risk from the second collision point to own aircraft's right at 70 deg. The display indicates that the predicted vertical separation can be increased by initiating a climb. Over a period of 10 s, the aircraft achieves a 5-deg climb angle and then maintains this angle. A small turn to the right at 0.15 deg per second is allowed. In this instance, the intruder does not change direction, being either uncooperative or unaware of the presence of own aircraft. The own aircraft display shows the main collision point drift down and to the left, as desired. The projected separation measures are seen to increase.

The situation at 10.1 s from the closest approach is shown in Fig. 3. The collision point is now about 20 deg below and 20 deg to the left. The crosshairs are now centered in the safer yellow/amber zone of the map. The miss distance is 1440 ft, with an upward component of 1130 ft and a sideways component of 460 ft. The conflict is thereby resolved. The horizontal miss distance could have been increased by turning own aircraft more to the right.

IV. Head-Up Display

As mentioned, a HUD is valuable in critical situations and in times of heavy pilot workload [11,16–18]. Typically, a HUD is superimposed on the pilot's field of view and is limited to monochromatic lines and simple symbols. Figure 4 is a HUD version of the zenithal MFD display. The crosshairs are limited in extent in the manner of the standard gun cross ([13], Fig. 46). The contours correspond to the EMDs of 1, 2, and 3 kft, which are the boundaries of the colored zones in the MFD display. Each contour is an analog of the ASE circle in Fig. 1. The collision point or zone is now represented by a dot and is the analog of the steering dot in the AARD. The LOS is shown as a solid square, though a hollow square could be retained. Both aircraft are flying level and own aircraft has a speed of 500 ft/s. The intruder has a speed of 400 ft/s, is at a distance of 6000 ft, and is 30 deg to the left and 7 deg below own aircraft. The intruder is crossing in front of own aircraft at 90 deg to own aircraft's path. The collision point could be reached in 10.7 s, but Fig. 4 shows that they would miss by about 1200 ft if neither aircraft maneuvered. This simple symbology, with some numbers attached, could be added to existing HUD symbology in the manner of existing combat displays [13,14].

Figure 5a shows the HUD version of Fig. 2, and Fig. 5b shows the HUD version of Fig. 3. Figure 5b illustrates contours resulting from the geometry in Fig. B2b. These displays could be used to resolve the conflict as described in Sec. III.

V. Comparative Evaluation of the Display Format

As mentioned, displays based on the same principles (Fig. 1) have proven very effective in providing military pilots with situational awareness in combat situations, which are the counterpart of civil aircraft conflict situations. This evidence is now supplemented by formulating a natural model of pilot response to the display and to TCAS displays. Computer simulation results with the model are reported, and some performance metrics are evaluated. It is noted that the computer simulation of human performance and response to the cockpit displays and other interfaces is an established methodology [21,22].

For a fair comparison, one considers a future in which the display information is accurate (unlike the current TCAS), and so only the nature of the display information is assessed. The successful avoidance by two aircraft is studied. Two cases are considered: the first, in which both pilots have the new display, and the second, in which both pilots have TCAS displays. It is supposed, in each case, that earlier avoidance maneuvers have failed and led to an emergency situation. The model pilot response to the new display is defined as follows:

1) A collision-imminent state is activated, and evasive action by the pilot is thenceforth guided by the new display. This occurs when the calculated time to the closest point of approach (CPA) falls to a preset value.

2) The pilot maintains a constant speed during evasive maneuvers.

3) The pilot steers so that the display crosshairs are moved normal to the contours of constant EMD in the direction of increasing EMD.

4) The collision-imminent state ceases when the CPA is reached. The pilot then ceases evasive action.

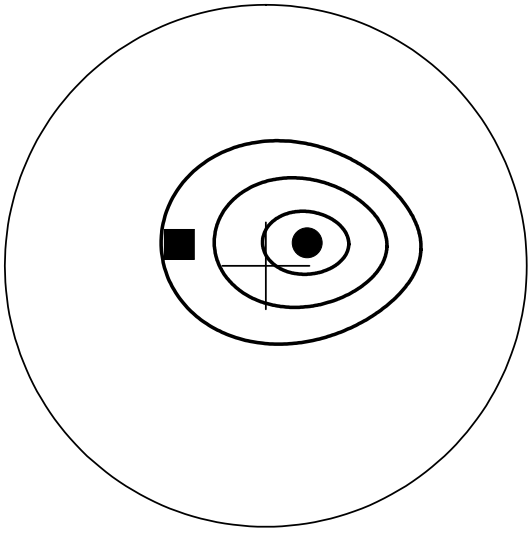

Fig. 4 A HUD display format matching the color display. It likewise shows the contours for EMDs of 1 kft, 2 kft, and 3 kft. The display crosshairs indicate an EMD of about 1.2 kft for the current aircraft speeds and directions. Numerical information could be added to match the color display or as required by different installations.

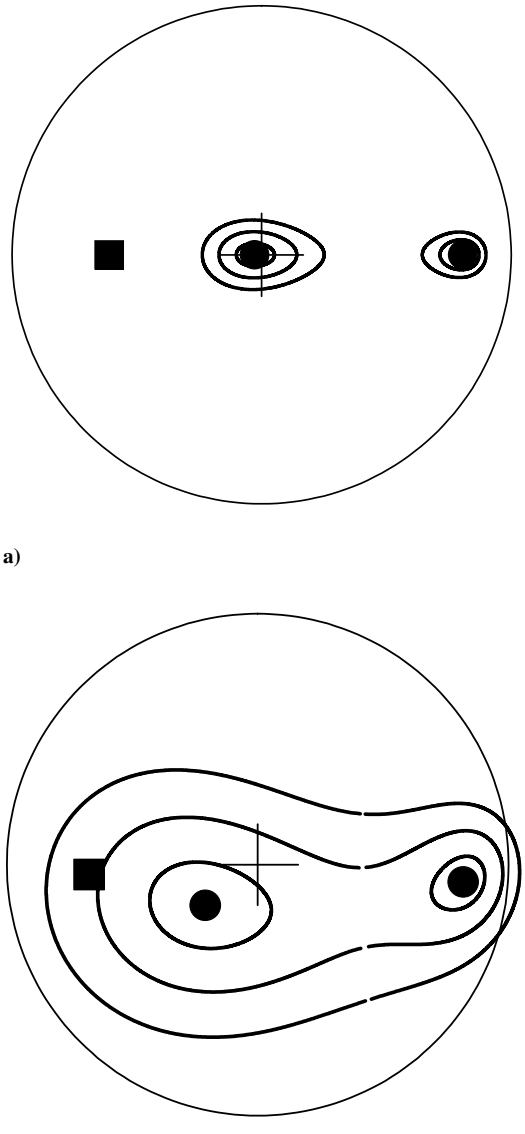

a)

b)

Fig. 5 The HUD display format of Fig. 4 for two times in a developing situation: a) corresponds to Fig. 2 and b) corresponds to Fig. 3.

There may have been state alerts before condition 1, but it is supposed that other operational factors have nevertheless led to a more serious conflict. Condition 2 recognizes that many aircraft might not be able to change speed significantly in a short time. Condition 3 has the effect of always increasing the EMD and is called *EMD steering*. Condition 4 excludes unnecessary evasion. Subsequently, the aircraft might resume their original courses. Incidentally, conditions 2 and 3 specify, in effect, a guidance law for the aircraft. Similar guidance laws have been suggested by Gazit and Powell [19] and by Zeghal [20] with application to automated guidance. They have shown that such laws have superior performance over some other proposed laws.

Coaltitude evasion by aircraft in level flight can cause difficulty for pilots, particularly on short time scales, and so this is an acid test of the new display. The current TCAS navigation display does not provide adequate visual guidance for pilots on the best direction for the turn. As mentioned, in a conflict a pilot's aim is to increase the miss distance, and the new display shows precisely how to do this. With the information in the current TCAS display, the pilot still must estimate how to do this on a heuristic basis. As shown in Appendix A, the turn direction depends in a complex way on three factors: the relative heading, the ratio of speeds, and the direction of the rotation of the LOS. Consequently, a pilot cannot always mentally compute the correct turn direction based on the TCAS display information. There is a predisposition that a pilot will follow the rules of the air [23] (RoA) insofar as they are definitive. A common and important scenario is two aircraft converging at a relative heading whose magnitude is more than 70 deg, neither having priority. Then, in a close encounter, a broad guideline is that both shall turn to the right. This propensity in behavior is supported by several studies [24,25]. The RoA are now used as a benchmark for evaluating the new display format.

A set of scenarios is constructed in which, on the contrary, the EMD response is for both aircraft to turn left. The purpose is to compare cases in which the EMD and RoA responses are different. There is a complementary set of cases in which the responses are the same, and so these are not included. First, aircraft having the same constant speed of 600 ft/s (355 kt) are considered. In each case, own aircraft is initially at 6 o'clock on a circle of radius 6000 ft and heading 10 deg to the left of center (Fig. 6). The intruder is initially on the circle, with its location at 1-deg steps around the circle but always at a minimum 70-deg relative heading with respect to own aircraft and heading for the center of the circle (Fig. 6). Thus, there are 221 cases. A similar set of cases was studied by Smith et al. [26].

Simple geometry shows that, if there were no maneuvers, the CPA would occur near the center of the circle with each aircraft having the other to its right. The EMD steering therefore directs both aircraft to turn left. The collision-imminent state is activated, and so avoidance commences. All turns are performed at a constant rate of 3 deg per second, a standard rate 1 turn under instrument flight rules. The initial separations are much smaller than those illustrated in Figs. 2 and 3, and the scales shown there would be reduced accordingly.

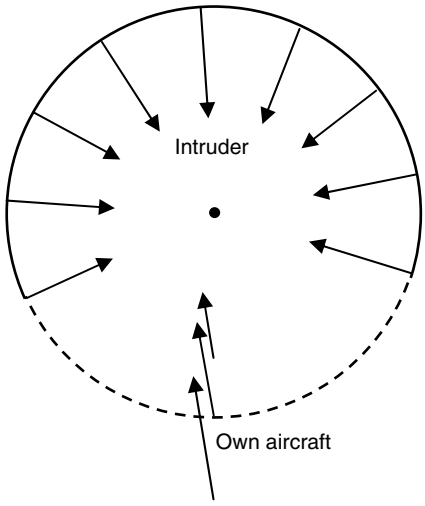

Fig. 6 Sketch of the initial own aircraft states and a sample of intruder states in the simulations.

Figure 7 illustrates the case in which the intruder starts due east of the center of the circle. No evasion would lead to a separation (center to center) of 740 ft at the CPA in 11 s. In Fig. 7a, both aircraft make EMD turns and diverge successfully after 9.6 s with a CPA separation of 2880 ft (when the collision-imminent state ceases). In Fig. 7b, both aircraft make RoA turns and diverge after 10.4 s, but with a smaller separation at a CPA of 1596 ft. In both figures, the aircraft are shown traveling in straight lines after the CPA, but this motion is chosen for simplicity and has no influence on the outcome of the resolution. Figure 7c shows the time-varying EMD, $R_{\mathrm{MD}}(t)$, in the two cases. For EMD turns, $R_{\mathrm{MD}}(t)$ increases throughout the resolution, but for RoA turns, $R_{\mathrm{MD}}(t)$ initially decreases to 0 at 1.8 s and then increases. *Thus, RoA turning initially makes matters worse and creates a collision course.* On the new display, these RoA turns would be clearly indicated as tending to move the crosshairs toward the collision point and would consequently be rejected.

Figure 8 shows the case in which the intruder starts due north on the circle, so that the aircraft are nearly head-on and the RoA explicitly demand that both aircraft turn right. No evasion by the aircraft would lead to a center-to-center separation at the CPA of 1046 ft in 10 s. EMD steering produces a separation at the CPA of 3845 ft after 8.9 s (Fig. 8a), whereas RoA steering produces a separation at the CPA of 1990 ft after 9.1 s (Fig. 8b).

Several performance metrics are considered. The separation, R_{CPA}, at the CPA is one measure of the success of the outcome. For a given initial situation, the time, t_{CPA}, to reach the CPA is a measure of inefficiency. During this time, the aircraft are still closing and still turning, and the conflict is not yet resolved. Thus, a large t_{CPA} is undesirable for two reasons. First, it implies prolonged task loading on pilots, which might lead them to make adverse decisions. Second, it produces large heading changes, which, at best, will require large heading changes to resume track and, at worst, might lead to conflicts with other aircraft. The simulation results show that, in every case, for EMD steering, R_{CPA} is greater, t_{CPA} is smaller, and $R_{\mathrm{MD}}(t)$ is greater for all t. Mean values of R_{CPA} and t_{CPA} over all cases (Table 1) are measures of performance, and both are subject to a minimum measure for acceptability. A small value of R_{CPA} in any single case would be unacceptable, and so the minimum of R_{CPA} over all cases is listed in Table 1. As Fig. 7c shows, RoA turns can steer aircraft across a collision course. This happens in every case, and so the number of such cases is $N_{\mathrm{Coll}} = 221$ (Table 1). For EMD turns, $N_{\mathrm{Coll}} = 0$ of course. All these statistics show the superiority of EMD steering over RoA steering. The mean t_{CPA} is not much smaller for EMD, but EMD could achieve the RoA value R_{CPA} by stopping the turns much earlier in each case.

For aircraft having different speeds, the speed ratio is of prime significance, and so different V_F are considered with V_T fixed at 600 ft/s. The same set of intruder initial conditions is used. In the first case, $V_F = 450$ ft/s (267 kt) with the aircraft again at 6 o'clock but only 4500 ft from the center of the circle (Fig. 6). In the second case, $V_F = 750$ ft/s (444 kt) with the aircraft again at 6 o'clock but 7500 ft from the center of the circle (Fig. 6). In both cases, the heading is 10 deg left of center, and a near miss would occur near the center in 10 s. Table 1 summarizes the results and shows the superiority of EMD steering over RoA steering in all cases.

In the complementary set of cases, where own aircraft's initial heading is 10 deg to the right of the center of the circle, EMD and RoA produce the same maneuvers. Thus, in the combined set of cases, EMD is never worse than RoA. The new display provides similar turning, climbing, and descending advice in 3-D, as illustrated in Sec. III. It is apparent from the previously mentioned simulation data that EMD maneuvers will produce a satisficing solution.

VI. Discussion

This section discusses aspects of the new display in the general context of cockpit display design. This is an active area of research

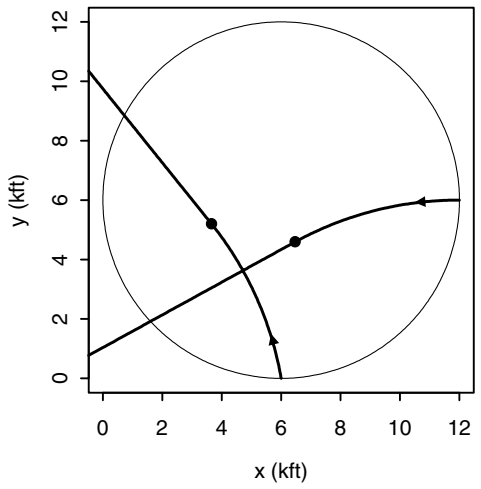

a)

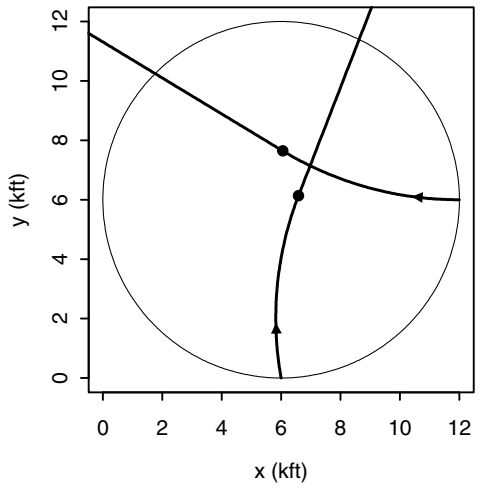

b)

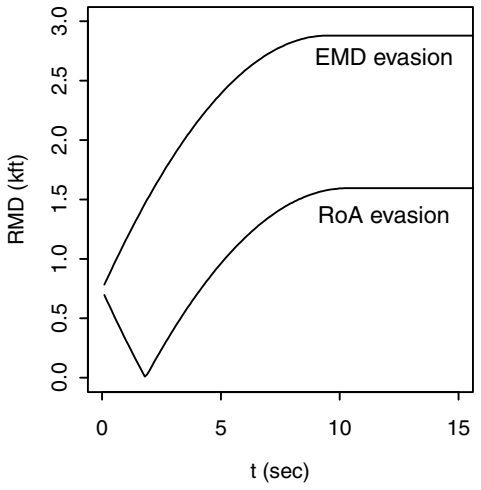

c)

Fig. 7 Aircraft paths and EMDs: a) Two aircraft evading by EMD steering, according to the new display, starting on the circle of Fig. 6. The dots show the locations at the CPA. b) Two aircraft evading by turning to the right, according to the RoA, starting on the circle of Fig. 6. The dots show the locations at the CPA. c) The evolving value R_{MD} of EMD with time for the two evasive maneuvers in Figs. 7a and 7b.

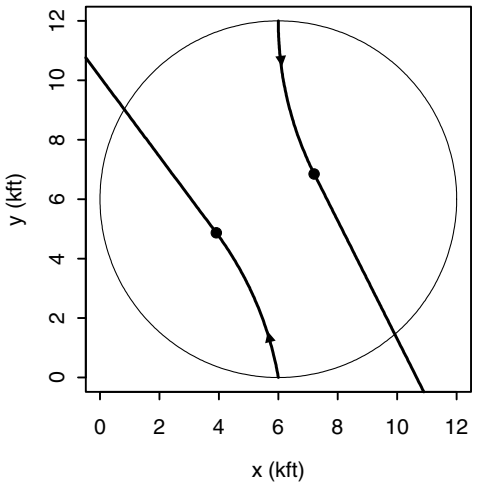

a)

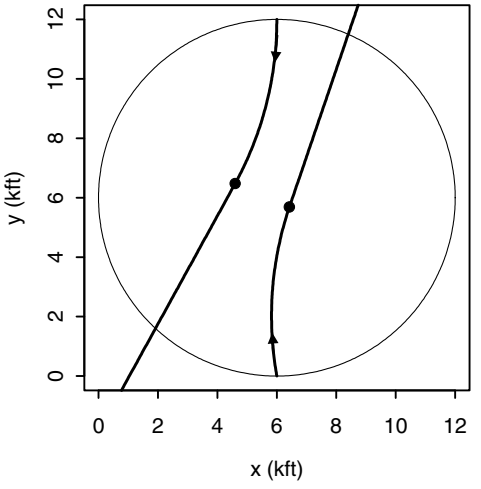

b)

Fig. 8 Aircraft paths: a) Two aircraft evading by EMD steering, according to the new display, starting on the circle of Fig. 6. The dots show the locations at the CPA. b) Two aircraft evading by turning to the right, according to the RoA, starting on the circle of Fig. 6. The dots show the locations at the CPA.

involving many complex and contentious issues. The research aims to overcome limitations of the current TCAS, as described in the Introduction.

Alexander and Wickens [5] studied a number of displays that augment the vertical-view VSD and the plan-view NAV display with a further vertical information display. These comprise three types: 1) 3-D perspective displays, 2) 2-D side-view displays, and 3) 2-D rear-view or forward-looking displays. The present format is nearest to type 3, with own aircraft at the center of the display. Alexander and Wickens showed that type 3 performs better than types 1 and 2 in flight simulation trials according to the following criteria: predicting conflict, safety of climbing maneuvers, lateral efficiency of climbing maneuvers, altitude maintenance, and efficiency of airspeed changes.

Krozel and Mogford [10] reviewed a large number of studies of pilot reactions to different experimental CDTI and reached similar conclusions. Plan views, such as that provided by the NAV display, are generally thought to provide insufficient vertical information. Pilots report difficulties in comprehending the information contained in 3-D perspective displays. Pilots also report difficulties in predicting future conflicts from these displays. These issues are addressed by the new display. First, it provides both vertical and horizontal information in an integrated form. Second, it avoids the complexity of 3-D perspective displays by projecting the essential 3-

Table 1 Performance metrics for EMD and RoA steering

V_F,ft/s	V_T, ft/s	Steering type	Mean R_{CPA}, ft	Mean t_{CPA}, s	Min R_{CPA}, ft	N_{Coll}
450	600	EMD	2748	9.02	1660	0
		RoA	1639	9.59	1051	221
600	600	EMD	3282	8.94	2048	0
		RoA	1703	9.67	960	221
750	600	EMD	3834	8.87	2513	0
		RoA	1775	9.72	911	221

D information in a form that has proven effective in combat aircraft. Third, potential future conflicts are explicitly predicted in the form of EMD and are displayed to the pilot.

A few display types illustrate some issues. Barhydt and Hansman [3] have augmented the NAV display by adding conflict bands and a new side view of the situation (type 2). As mentioned, the conflict bands have some similarities to the present color contours. Their display uses information or predictions about the intended future motion of the other aircraft. Evidently, such information is valuable if it is completely reliable, and their study confirms this. However, displays that include intent carry a risk that pilots will place undue confidence in unreliable predictions with serious consequences. This risk would need to be assessed.

One innovative class of display designs is known as *pathway* [27], *tunnel* [28], or *highway* [29] *in the sky*. Kramer et al. [30] evaluated the influence of different pathway and guidance delay concepts using a head-up version of such a display. The method computes a safe future pathway for an aircraft based on a model of probable intruder motions. The pathway is displayed as a 3-D perspective view superimposed on a 3-D scene (type 1). The utility of the display relies on three factors: the correctness of the assumptions in the underlying model, the complete and intuitive understanding of these assumptions by pilots, and the ability of pilots to interpret the 3-D perspective information. By contrast, the new display format proposed here identifies the *unsafe* directions and gives the pilot more flexibility in choosing safe directions. Thus, it provides information of a similar type in a less complex display and the information is not dependent on complex assumptions.

Knecht and Smith [31] have patented a display concept that involves a forward 2-D view (type 3), though not a stereographic projection. They compute and display a safe zone at a chosen time horizon. The zone is based on a model for possible future maneuvers by other aircraft. In this sense, it resembles the pathway-in-the-sky displays. It likewise involves assumptions, but the display is much simpler. A disadvantage is that the safe zone develops too rapidly with time, and so the time horizon needs to be regularly reset. The new display evolves more smoothly, as shown.

The computations behind some of these displays are substantial and involve numerical, iterative algorithms. It is difficult to prove that such algorithms converge to correct solutions in all possible scenarios. Then there is a risk that occasionally the display cannot be computed or is incorrect, perhaps in critical situations. By contrast, the new displays are computed from relatively simple, explicit, closed formulas. This means that the computations are reliable.

Displays are sometimes evaluated by their inventors in physical simulators, with a small number of pilot crews and a small number of scenarios. There are significant problems with the rigorous experimental design and analysis of such a trial. Some conclusions are based on questionnaires about what pilots prefer, but these tend to be biased toward what pilots are familiar with. Other conclusions are based on analyses of pilot responses in simulated conflict situations, but again there is a bias toward the familiar. The purpose is to test the display–pilot interface, but variability in the pilot–aircraft interface is difficult to separate out and assess. There is also the danger that situations are chosen, perhaps unintentionally, to favor features of a new design, with a consequent bias in favor of that design. There is a potential bias in the selection of pilots. For the displays presented here, one might prefer to use pilots with combat experience, but this might bias the results. Personal biases and the effects of variability tend to be reduced by careful experimental design in large-scale, comparative studies [5] performed by specialists. Such a study is well beyond the scope of the present paper. However, for the many reasons given, the present display format should perform well in such a study.

VII. Conclusions

A new type of display format has been described based on projecting the sphere of directions around own aircraft onto a plane. The LOS of an intruder and the collision directions for own aircraft then appear as extended points on the display. A principal innovation is the use of EMD to create a color-coded map, or monochrome contours suitable for a HUD. These features are designed to provide the pilot with a very intuitive and immediate impression of the level of danger in a close encounter and a clear guide for steering out of danger. The main observations are as follows:

1) Situational data and displays in civil aircraft can be enhanced significantly.

2) The new display format takes full advantage of advances in A/A data links and onboard navigation systems, including GPS.

3) The basic functionality of the new display format has long been proven in military aircraft display design.

4) The direct display of EMD relieves the pilot of the task of predicting the outcomes of alternative actions that might be chosen, in contrast with the current TCAS.

5) Horizontal and vertical information are displayed as one, whereas TCAS uses two displays.

6) The display format avoids the complexity of 3-D perspective displays but contains the essential 3-D information required to resolve a close conflict.

7) In close encounters, simulations show that steering directions indicated by the display produce better outcomes than conventional steering.

There is scope for modifying and adding many features to the displays. Other types of projections that might be useful include an equal area for an equal solid angle [4] or simple normal projections. The latter have the advantage of giving more weight to the center of the display. One could develop options and algorithms for resizing or rescaling collision zones and for selecting a subset of directions, as currently available in the AARD. One could also add symbols based on the possibility of dangerous turning by the intruder. The aircraft simulation model in the animation program could be replaced by realistic simulations with 6 degrees of freedom for various types of aircraft. For conflicts between ships, the same methods provide displays of 2-D directions.

Appendix A: Calculating Extrapolated Miss Distance and Collision Points

EMD is a commonly calculated quantity, but other vectors and components are required in Appendix B, and so the calculation is outlined here. The collision geometry is sketched in Fig. A1a. Own aircraft has a 3-D velocity vector, $\mathbf{V}_F$; the intruder has a 3-D velocity vector, $\mathbf{V}_T$; their current 3-D distance is R_0; and the LOS to the intruder is given by the unit vector $\mathbf{U}_{LOS}$. Here, F is for first person and T is for intruder or threat or traffic. From the point of view, or frame of reference, of the intruder, own aircraft appears to move with the velocity $\mathbf{V}_R = \mathbf{V}_F - \mathbf{V}_T$ in a direction with the unit vector $\mathbf{U}_R = \mathbf{V}_R/|\mathbf{V}_R|$ if $\mathbf{V}_F \neq \mathbf{V}_T$. Figure A1b shows that the EMD is the shortest distance from the intruder to the line through own aircraft in

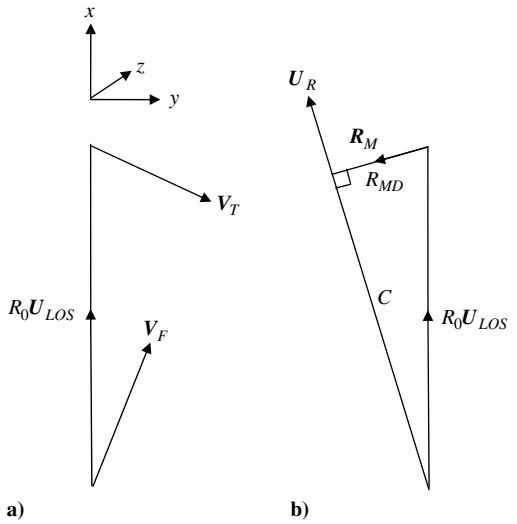

Fig. A1 Velocity vectors and miss distance: a) An example of a situation. The axes x and y are chosen to lie in the plane of $\mathbf{V}_T$ and $\mathbf{U}_{\mathrm{LOS}}$, but $\mathbf{V}_F$ need not lie in this plane. b) Illustrates the calculation of R_{MD}.

the direction of $\mathbf{U}_R$. The shortest path is the perpendicular to the line. The component of the relative position vector $R_0\mathbf{U}_{\mathrm{LOS}}$ along $\mathbf{U}_R$ is $C = R_0\mathbf{U}_{\mathrm{LOS}} \cdot \mathbf{U}_R$, where the dot denotes the scalar product. If $\mathbf{V}_F = \mathbf{V}_T$, then $C = 0$. Hence, the vector from the intruder to own aircraft at closest approach would be

$$\mathbf{R}_M = C\mathbf{U}_R - R_0\mathbf{U}_{\mathrm{LOS}} \tag{A1}$$

Pythagoras's theorem gives the EMD as

$$R_{\mathrm{MD}} = |\mathbf{R}_M| = \sqrt{R_0^2 - C^2} \tag{A2}$$

This formula is used to compute the EMDs for all hypothetical own aircraft directions, creating the color displays in Figs. 2 and 3. For own aircraft's current velocity vector, the component H_M of $\mathbf{R}_M$ along the upward axis and the component W_M along the right wing are also calculated. They show how far own aircraft will pass above and to the right of the intruder at closest approach, and their values are given next to the arrows in the bottom of the display (Figs. 2 and 3).

The collision points correspond to $R_{\mathrm{MD}} = 0$, which occurs when $\mathbf{U}_R = \mathbf{U}_{\mathrm{LOS}}$ as Eq. (A2) shows, so that $\mathbf{U}_{\mathrm{LOS}}$, $\mathbf{V}_F$, and $\mathbf{V}_T$ are coplanar. Orthogonal coordinates (x, y, z) are chosen in which the x axis lies along $\mathbf{U}_{\mathrm{LOS}}$ and the y axis lies in the plane of $\mathbf{U}_{\mathrm{LOS}}$ and $\mathbf{V}_T$, such that $\mathbf{V}_T$ has a positive y component, V_{Ty}. The z axis is defined by the right-hand rule. The collision triangle shown in Fig. A2a shows a case in which $V_F > V_T$. Otherwise, Pythagoras's theorem gives the standard formula

$$|\mathbf{V}_R| = -V_{Tx} + \sqrt{V_F^2 - V_{Ty}^2} \tag{A3}$$

and the own aircraft velocity vector would be

$$\mathbf{V}_{F1} = \mathbf{V}_T + |\mathbf{V}_R|\mathbf{U}_{\mathrm{LOS}} \tag{A4}$$

Figure A2b illustrates a case in which $V_F < V_T$ and there are two collision directions. Clearly this can happen only if V_{Tx} is negative. For the second, the plus before the square root in Eq. (A3) becomes a minus. This gives a second own aircraft velocity vector, $\mathbf{V}_{F2}$. The directions of these vectors correspond to the centers of the white zones in Figs. 2 and 3. The distances, C, and times, $C/|\mathbf{V}_R|$, to these collision points are attached to the locations in the display.

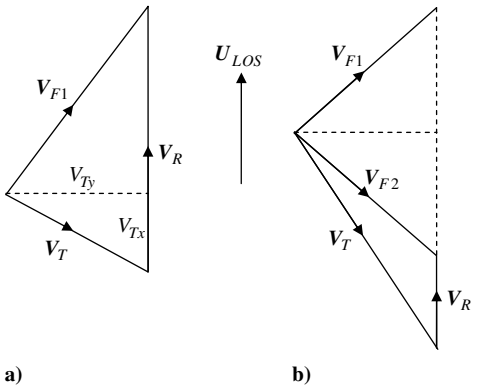

Fig. A2 Velocity vectors for collisions: a) A collision triangle for a situation in which $V_F > V_T$ leading to a single aircraft collision velocity vector $\mathbf{V}_{F1}$. b) When $V_F < V_T$, there can be two aircraft collision velocity vectors $\mathbf{V}_{F1}$ and $\mathbf{V}_{F2}$.

Appendix B: Equations and Shapes of Head-Up Display Contours

One can use the computer program to obtain a contour of fixed EMD, pixel by pixel, but this is computationally expensive and does not generate a smooth curve. Instead, an equation for the contour is obtained, referring to the collision geometry in Fig. A1a. Equation (A2) can be written in the form

$$(R_0\mathbf{U}_{\mathrm{LOS}} \cdot \mathbf{V}_R)^2 = (R_0^2 - R_{\mathrm{MD}}^2)|\mathbf{V}_R|^2 \tag{B1}$$

which can be expressed in components as

$$R_0^2 V_{Rx}^2 = (R_0^2 - R_{\mathrm{MD}}^2)(V_{Rx}^2 + V_{Ry}^2 + V_{Rz}^2) \tag{B2}$$

The hypothetical own aircraft velocity is written as $\bar{\mathbf{V}}_F = (X, Y, Z)$, where the components X, Y, and Z are variables that will define the contour. Then,

$$V_{Rx} = X - V_{Tx} \qquad V_{Ry} = Y - V_{Ty} \qquad V_{Rz} = Z \tag{B3}$$

because $\mathbf{V}_T$ has no z component due to the choice of axes. Now Eq. (B2) reduces to

$$\beta^2(X - V_{Tx})^2 = (Y - V_{Ty})^2 + Z^2 \tag{B4}$$

where

$$\beta = \sqrt{\frac{R_{\mathrm{MD}}^2}{R_0^2 - R_{\mathrm{MD}}^2}} \tag{B5}$$

Equation (B4) defines a cone with the vertex $\mathbf{V}_T$, the axis along the x axis, and the semi-angle $\theta = \arctan\beta$. Figure B1 shows one example. Recalling that own aircraft's actual current speed, $V_F \equiv |\mathbf{V}_F|$, is assumed for all hypothetical own aircraft directions gives

$$X^2 + Y^2 + Z^2 = V_F^2 \tag{B6}$$

This defines the surface of a sphere of radius V_F, centered at the origin, as illustrated in Fig. B1. The simultaneous Eqs. (B4) and (B6) define two closed curves, where the cone intersects the sphere. The hypothetical own aircraft velocities, $\bar{\mathbf{V}}_F = (X, Y, Z)$, then lie on these curves (Fig. B1). Also, the collision points lie at the intersection of the axis of the cone with the surface of the sphere, because $\beta = 0$ when $R_{\mathrm{MD}} = 0$. The $\bar{\mathbf{V}}_F$ have directions given by the unit vector $\bar{\mathbf{U}}_F = \bar{\mathbf{V}}_F/V_F$. To plot the projections of the $\bar{\mathbf{U}}_F$, one first writes Eq. (B4) in the parametric form:

$$X - V_{Tx} = h \qquad Y - V_{Ty} = h\beta\cos\phi \qquad Z = h\beta\sin\phi \tag{B7}$$

where h is the vertical distance above the vertex of the cone and ϕ is the polar angle around the axis of the cone (Fig. B1). Substituting this in Eq. (B6) gives the quadratic equation for h:

$$h^2(1 + \beta^2) + 2h(V_{Tx} + V_{Ty}\beta\cos\phi) + (V_T^2 - V_F^2) = 0 \tag{B8}$$

The two solutions are denoted $h_+(\phi)$ and $h_-(\phi)$. When $h_+(\phi)$ is substituted in Eq. (B7), one gets the equation of the upper curve in

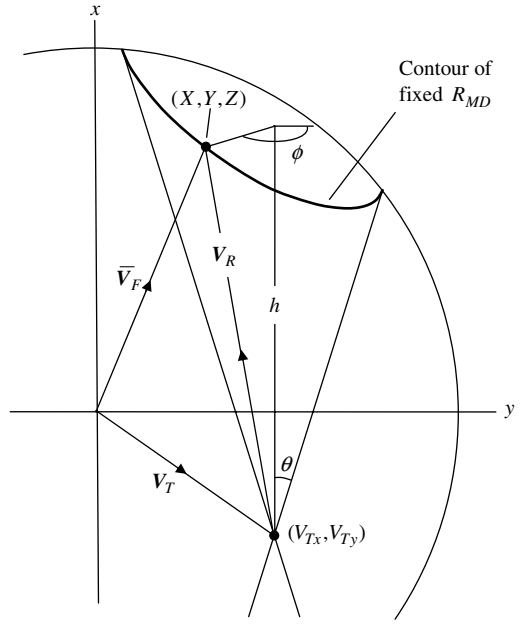

Fig. B1 Construction of a contour of fixed R_{MD} for a monochrome display or a HUD.

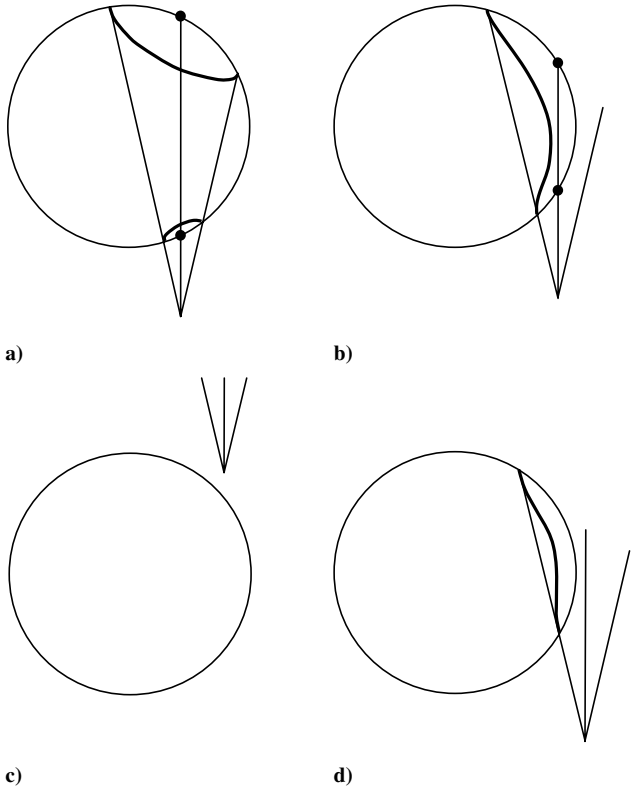

Fig. B2 Illustration of different states of a contour: a) two collision points within separate contours; b) two collision points within one contour; c) no collision point and no contour, faster intruder in retreat; and d) no collision point but a single contour. Figure is the case of one collision point and one contour.

Fig. B1 expressed in terms of the single parameter ϕ. One can generate the curve from Eq. (B7) by stepping through closely spaced values of ϕ in the range $(0, 2\pi)$. The directions $\bar{\mathbf{U}}_F$ are then projected zenithally [4], for three values of R_{MD}, to produce Fig. 4.

A lower curve in Fig. B1 could be obtained from $h_{-}(\phi)$ in the same way. However, the lower half of the cone corresponds to a minimum separation occurring in the past, and so it is not physically relevant. In a case such as Fig. B2a, however, both curves lie on the upper half of the cone and occur in the future. The resulting projection produces two contours, as in Fig. B2a. The possible situations are as follows. If own aircraft is faster ($V_F \geq V_T$), there is exactly one collision point. This follows because the vertex of the cone is inside the sphere in Fig. B1. If own aircraft is slower ($V_F < V_T$), then the vertex is outside the sphere and there are two main cases:

1) If $V_{Tx} > 0$, there is no collision point, because the vertex of the cone lies above the sphere (Fig. B2c). If $V_{Tx} < 0$ and $V_{Ty} > V_F$, there is no collision point, because the vertex of the cone lies to the side of the sphere (Fig. B2d). In both cases, if V_T is large enough, there is no contour either.

2) If $V_{Tx} < 0$ and $V_{Ty} < V_F$, there are two collision points, because the vertex of the cone lies below the sphere (Figs. B2a and B2b). There is always at least one contour. A single contour, which could be dumbbell shaped, can enclose both collision points (Fig. B2b). Or two separate contours can each contain one collision point (Fig. B2a). Unless $V_F \ll V_T$, one collision point is much closer and has a much larger contour. The mathematical conditions for the different types of contours can be deduced from these figures.

Acknowledgments

The authors express their appreciation that this work, as part of a broader safety program, has received interest, support, and review by Murray Warfield (QANTAS Airways Limited), Scotty Fairbairn (Aviation Standards International), and Terry Wesley Smith (Chief Executive Officer, Regional Aviation Association of Australia).

References

[1] Love, W. D., "TCAS III: Bringing Operational Capability to Airborne Collision Avoidance," *AIAA/IEEE 8th Digital Avionics Systems Conference*, AIAA, Washington, D.C., 1988, pp. 887–881.

[2] Scallen, S. F., Smith, K., and Hancock, P. A., "Pilot Actions During Traffic Situations in a Free-Flight Airspace Structure," *Proceedings of the Human Factors and Ergonomics Society 40th Annual Meeting*, Human Factors and Ergonomics Society, Santa Monica, CA, 1996, pp. 111–115.

[3] Barhydt, R., and Hansman, J., "Experimental Studies of the Effect of Intent Information on Cockpit Traffic Display," Massachusetts Institute of Technology Rept. ASL-97-3, Cambridge, MA, 1997.

[4] Helleberg, J., Wickens, C. D., and Xu, X., "Pilot Maneuver Choice and Safety in a Simulated Free Flight Scenario," Univ. of Illinois Inst. of Aviation TR ARL-00-1/FAA-00-1, Jan. 2000.

[5] Alexander, A. L., and Wickens, C. D., "Cockpit Display of Traffic Information: The Effects of Traffic Load, Dimensionality, and Vertical Profile Orientation," *Proceedings of the 45th Annual Meeting of the Human Factors and Ergonomic Society*, Human Factors and Ergonomics Society, Santa Monica, CA, Oct. 2001, pp. 105–109.

[6] Hardy, G. H., and Lewis, E. K., "Cockpit Display of Traffic and Wake Information for Closely Spaced Parallel Approaches," AIAA Paper 2004-5106, Aug. 2004.

[7] Kovari, B., "More Effective Usage of Airspace," *Periodica Polytechnica. Transportation Engineering*, Vol. 29, Nos. 1–2, 2001, pp. 101–106.

[8] Alexander, A. L., Wickens, C. D., and Merwin, D. H., "Perspective and Coplanar Cockpit Displays of Traffic Information: Implications for Maneuver Choice, Flight Safety, and Mental Workload," *International Journal of Aviation Psychology*, Vol. 15, No. 1, 2005, pp. 1–21. doi:10.1207/s15327108ijap1501_1

[9] Pritchett, A. R., and Hansman, R. J., "Experimental Studies of Pilot Performance at Collision Avoidance During Closely Spaced Parallel Approaches," *Proceedings of the 9th International Symposium on Aviation Psychology*, 1997, pp. 1083–1088.

[10] Krozel, J., and Mogford, R., "Free Flight Literature Survey: Human Factors Research Using Empirical Studies," *Eleventh International Symposium on Aviation Psychology*, Ohio State Univ. Press, Columbus, OH, May 2001.

[11] Downs, E. (ed.), *Jane's Avionics 2004–2005*, Jane's Information Group, Coulsdon, Surrey, U.K./Alexandria, VA, 2004.

[12] Geiselman, E. E., and Post, D. L., "Helmet-Mounted Display Targeting Symbology Color Coding: An Air-to-Air Scenario Evaluation," Helmet- and Head-Mounted Displays IV, edited by R. J. Lewandowski, L. A. Haworth, W. Stephens, and H. J. Girolamo, International Society for Optical Engineering, Bellingham, WA, 1999, pp. 66–75.

[13] "Military Interface Standard: Aircraft Display Symbology," U.S. Air Force, U.S. Department of Defense, MIL-STD-1787B, April 1996.
[14] Shaw, R. L., *Fighter Combat: The Art and Science of Air-to-Air Warfare*, 2nd ed., Patrick Stephens Limited, United Kingdom, 1988.
[15] Hinks, A. R., *Map Projections*, 2nd rev. ed., Cambridge Univ. Press, Cambridge, England, U.K., 1921.
[16] Wong, D. T., Kramer, L. J., and Norman, R. M., "Two Aircraft Head-Up Traffic Surveillance Symbology Issues: Range Filter and Inboard Field-of-View Symbology," NASA Langley Research Center Rept. L-18102, NAS 1.15211037, TM-2001-211037, 2001.
[17] Snow, M. P., Reising, J. M., Liggett, K. K., and Barry, T. P., "Flying Complex Approaches Using a Head-Up Display: Effects of Visibility and Display Type," *10th International Aviation Psychology Symposium*, Ohio State Univ. Press, Columbus, OH, 1999.
[18] Fadden, S., Wickens, C. D., and Ververs, P. M., "Costs and Benefits of Head-Up Displays: An Attention Perspective and a Meta Analysis," *2000 World Aviation Congress*, Society of Automotive Engineers, Paper 2000-01-5542, 2000.
[19] Gazit, R. Y. and Powell, J. D., "Aircraft Collision Avoidance Based on GPS Position Broadcasts," *15th AIAA/IEEE Digital Avionics Systems Conference*, AIAA/IEEE, Omnipress, Madison, WI, Oct. 1996.
[20] Zeghal, K., "A Comparison of Different Approaches Based on Force Fields for Coordination Among Multiple Mobiles," *Proceedings of the 1998 IEEE/RSJ International Conference on Intelligent Robots and Systems*, 1998, pp. 273–278.
[21] Corker, K., and Smith, B., "An Architecture and Model for Cognitive and Engineering Simulation Analysis: Application to Advanced Aviation Automation," *Proceedings of the 9th AIAA Computing in Aerospace Conference*,IEEE/RSJ International, Omnipress, Madison, WI, Oct. 1993, pp. 1079–1088.
[22] Duley, J., Miller, C., Schultz, E., and Hannen, M., "A Human Resource-Based Crew Station Design Methodology," *Proceedings of the 13th Digital Avionics Systems Conference*, AIAA/IEEE, Omnipress, Madison, WI, Nov. 1994, pp. 233–238.
[23] "Annex 2: Rules of the Air," *Convention on Civil Aviation*, 9th ed., International Civil Aviation Organization, July 1990, Chap. 3.
[24] Beringer, D. B., "Collision Avoidance Response Stereotypes in Pilots and Nonpilots," *Human Factors*, Vol. 20, No. 5, 1978, pp. 529–536.
[25] Merwin, D. H., and Wickens, C. D., "Evaluation of Perspective and Coplanar Cockpit Displays of Traffic Information to Support Hazard Awareness in Free Flight," Univ. of Illinois Inst. of Aviation TR ARL-96-5/NASA-96-1, 1996.
[26] Smith, J. D., Ellis, S. R., and Lee, E. C., "Perceived Threat and Avoidance Maneuvers in Response to Cockpit Traffic Displays," *Human Factors*, Vol. 26, No. 1, 1984, pp. 33–48.
[27] Newman, R. L., and Mulder, M., "Pathway Displays: A. Literature Review," *Proceedings 22nd Digital Avionics Systems Conference*, AIAA/IEEE, Omnipress, Madison, WI, Oct. 2003, pp. 9.D.6-1–9.D.6-10.
[28] Mulder, M., and van der Vaart, H. J. C., "An Information Centred Analysis of the Tunnel-in-the-Sky Display, Pt. 3: Curve Interception," *International Journal of Aviation Psychology*, Vol. 16, No. 1, Jan. 2006, pp. 21–49. doi:10.1207/s15327108ijap1601_2
[29] McKinley, J. B., Heidhausen, E., Kramer, J. A., and Krone, N. J., "Flight Testing of an Airborn SVS with Highway-in-the-Sky on a Head-Up Display," *24th Digital Aviation Conference*, AIAA/IEEE, Omnipress, Madison, WI, 2005, pp. 13.C.1-1–13.C.1-9.
[30] Kramer, L. J., Prinzel, L. J., III, Arthur, J. J., III, and Bailey, R. E., "Advanced Pathway Guidance Evaluations on a Synthetic Vision Head-Up Display," *National Aeronautics and Space Administration*, NASA TP 2005-213782, July 2005.
[31] Knecht, W. R., and Smith, C., "Flight Information Computation and Display," U.S. Patent No. 6,970,104 B2, 29 Nov. 2005.